Applied Organometallic Chemistry WILEY

Vanadium metal complexes' inhibition studies on enzyme PTP-1B and antidiabetic activity studies on Wistar rats

Ayub Shaik[1] | **Vani Kondaparthy**[1] | **Rambabu Aveli**[2] |
Louwkhyaa Vemulapalli[1] | **Deva Das Manwal**[1]

[1]Department of Chemistry, Osmania University, Hyderabad, India

[2]Department of Science and Humanities, St. Martin's Engineering College, Hyderabad, India

Correspondence
Ayub Shaik, Department of Chemistry, Osmania University, Hyderabad 500007, Telangana, India.
Email: drayubsk@osmania.ac.in

Evidence from biochemical, genetic, and pharmacological studies strongly suggest that inhibition of protein tyrosine phosphatase-1B (PTP-1B) enzyme could address both diabetes and obesity and thus making PTP-1B as an exciting target for drug development. Although many natural PTP-1B inhibitors showed promising clinical and potential activity, still there is no clinically used PTP-1B inhibitor which is most likely due to relatively low activities or lack of selectivity. With this background, we have synthesized and characterized the inhibitors exclusive for PTP-1B. Vanadium metal complexes were our choice. The purpose of this investigation is twofold: firstly, to evaluate the inhibitory properties of these vanadium metal complexes on enzyme PTP-1B and secondly, to know the ease with which these metal complexes are being transported by transporting proteins like bovine serum albumin (BSA). To synchronize these results, experiments on induced diabetic Wistar Rats were conducted. Also, we evaluated the PTP-1B inhibitory effects of these vanadium metal complexes theoretically (molecular modeling) and experimentally (enzyme kinetics) and found that they have excellent inhibitory properties on PTP-1B. These complexes upon injecting reduced the serum glucose levels to normal range in induced diabetic Wistar rats within 3 days of experiments. The order of glucose reducing properties of these metal complexes from different experiments is found to be the same. Among these complexes, [7-imi], which is derived from [Bis(1,-3-diphenyl-1,3propanedione)oxovanadium (IV)] and imidazole as ligands, has shown to be more effective in in vitro and in vivo studies compared with methyl imidazole and ethyl imidazole.

KEYWORDS
drug-protein interaction and quenching, kinetic study, PTP-1B, serum glucose, vanadium complex

1 | INTRODUCTION

Increased incidence of type 2 diabetes (T2D) and obesity has elevated the medical need for new agents to treat the disease states. Resistance to the hormone insulin and leptin are hallmarks of both T2D and obesity. The discovery in 1899 by Lyonnet and Martin[1] that diabetic patients excreted less glucose in their urine after

treatment with vanadate indicated that transition metal compounds may have an important role to play in the treatment of DM. It was shown that $NaVO_3$ (sodium vanadate) does not enhance insulin action in type 1 diabetes but selectively improves insulin action in T2D patients. Vanadium has been demonstrated to mimic insulin in treating DM.[2] Compared with inorganic vanadium salts, complexes of vanadium with appropriate organic ligands can improve absorption, tissue uptake, potency, and decrease the toxicity of the metal.[3] An organic vanadyl derivative [bis (maltolato) oxovanadium (IV)] is currently on phase II clinical trial as an antidiabetic drug.[4] The most potent form of vanadium is with the combination of maltol in 1:2 ratio resulting in water soluble and neutral vanadium metal complex, [(VO (MA)2] where MA = maltol, known as bis (maltolato) oxovanandium (IV), a proven insulin enhancing agent.[4a] The insulin-sensitizing effect of vanadium complex $Na_2[VO (Glu)_2(CH_3OH)]$ (Glu = glutamate) has the ability to inhibit protein tyrosine phosphatases (PTPs).[4b] Chelates of oxovanadium (IV) with acetylacetone ligand [i.e., Bis (acetylacetonato) oxovanadium (IV)] are known to lowering blood glucose levels.[4c–f] Organic chelates of VO enhanced insulin-mimetic action compared with that of VOSO4.[4g] So, the vanadium metal complex with organic ligands instead of pure different vanadyl salts offers a far more versatile means of delivering the metal.

Owing to the importance of vanadium metal complexes in biology, in earlier papers,[5,6] we have reported the synthesis and characterization of few vanadium metal complexes using different substituted acetylacetones. By taking all these points into consideration, the properties of the metal complex may be improved by the correct choice of ligand and useful therapeutic effect may be achieved at lower doses.

Before performing inhibitory studies on the PTP-1B enzyme, we thought it would be better to have studies on the interaction of these complexes with human serum albumins (HSA) because of their biological role in carrying these metal complexes into the cell. For this purpose, bovine serum albumin (BSA) has been chosen instead of HSA.

PTPases are a large family of enzymes with regulations of the innumerable cellular processes by dephosphorylating proteins in living organisms. Four human PTPases[7] are PTP-1B, TCPTP, HePTP, and SHP-1. Among these PTPases, the enzyme PTP-1B acts as a key negative regulator of insulin[8,9] signaling through directly inactivating insulin receptor (IR) by dephosphorylating tyrosine residues in the regulatory domain. The perfect coordination between the action of two (Protein Tyrosine Kinase - PTK and PTP - PTP [i.e., phosphorylation and dephosphorylation]) proteins is the essence of the mechanism of opening and closing the cell doors for glucose intake.[10] Overactive PTPases disturb the concerted action between PTK and PTP which is essential for opening and closing of the cell doors, making the cell wall not to respond to insulin. It has been established that oxidovanadium (IV) compounds have inhibitory action on PTPases[11–14]; as a result, the phosphoester bond is not broken; thus, signal transduction remains intact allowing glucose to enter the cell.

With this background of information, we were interested in testing the inhibition ability of these vanadium complexes on the overactive enzyme PTP-1B which is an active partner in glucose metabolism in living organisms, and the kinetic experiments were designed for this purpose.

2 | EXPERIMENTAL

2.1 | Materials and instrumentation

Vanadium metal complexes, shown in Figure 1, which were reported early,[5] abbreviated as [7-B], [7-imi], [7-me-imi], and [7-et-imi] were prepared and characterized in our lab. Enzyme PTP-1B was obtained from Cell Sciences, Newburyport, MA 01950, USA. p-Nitrophenylphosphate (pNPP) of analytical reagent grade obtained from Sisco Research Laboratories Pvt Ltd. Tris buffer of analytical reagent grade was obtained from Finar and used without further purification. BSA was purchased from Sigma-Aldrich.

The following instruments were used to perform different experiments: Spectrophotometer (EPOCH-BioTek, SN 1701311.), JASCO spectrofluorometer FP-8500, 96 microwell plate readers, and Shimadzu IR Prestige-21 spectrophotometer.
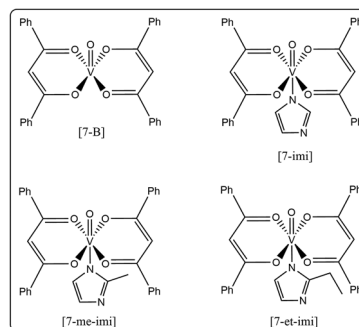

FIGURE 1 Structures of test compounds (previously reported)

2.2 | Methods

2.2.1 | BSA binding studies of vanadium complexes by fluorometric emission technique

The fluorescence spectra of BSA were recorded in the absence and presence of an increasing concentration of vanadium metal complexes in the wavelength range of 250–500 nm. BSA was used in buffer solution[15] (containing 5 mM Tri HCl/50 mM NaCl at pH 7.2). The spectra were recorded by exciting the BSA at 278 nm with the excitation and emission slit width of 5 nm and maximum emission found at 338 nm. The fluorescence titrations were carried out manually by adding various concentrations of the vanadium metal complexes to the 3 ml of BSA solution of 4.3 μM (fixed). The detailed protocols on the concentration of BSA and different concentrations of metal complexes along with other relevant calculated values are given in Tables S1–S3.

2.2.2 | Enzyme kinetics

Optimization of reaction conditions
To produce an effective enzyme assay, the optimal condition for the particular reaction has to be evaluated so that the maximum product can be obtained. The following have been used to determine various optimal conditions such as maximum absorption (λ_{max}), maximum temp, pH, the concentration of reactants, the concentration of enzyme, and the concentration of inhibitor for the reaction "hydrolysis of pNPP by PTP-1B enzyme" to obtain a maximum product of maximum OD. The determined optimal conditions for the "hydrolysis of pNPP by PTP-1B enzyme" are as follows: $\lambda_{max} = 405$ nm, $T = 27°C$, pH = 7.5, [E] = 40 nM, [S] = 15 mM, [I] = 10 μM. Once the optimal conditions for pNPP catalytic activity were determined, the enzyme kinetics can be studied. The protocol followed as in previous literature.[16–18]

The protocol followed for hydrolysis of pNPP in presence of PTP-1B
Different concentrations (5, 7.5, 15, 30, and 50 mM) of the substrate (pNPP) were prepared and taken in different test tubes. A fixed concentration (40 nM) of the enzyme was prepared in a buffer (tris pH = 7.5), was added to each test tube, and incubated at 27°C for 30 minutes. The assays were terminated by the addition of 5 μl of 10 M NaOH. The absorbance at 405 nm was measured on a 96 well microplate reader, and the recorded values were taken as "soft data" (Table S4). Same soft data were generated two more times in the above manner. Soft data generated by microplate reader contains absorbance (A) or OD at different time intervals for different concentrations of substrates.

The protocol followed for hydrolysis of pNPP in presence of PTP-1B and inhibitor
This reaction was carried out in the presence of a fixed concentration (5 μM) of inhibitor, keeping the rest of the things the same as mentioned in the above section.

2.2.3 | Molecular modeling studies of metal complexes with enzyme PTP-1B and BSA

Theoretical studies would be much useful to correlate the experimentally obtained data. Hence, molecular modeling on PTP-1B and BSA were performed. The interaction of the proteins BSA and PTP-1B with the different vanadium compounds was studied using molecular docking. The crystal structure of PTP-1B enzyme was retrieved from the Protein Data Bank (PDB) of the Research Collaboration for structural Bioinformatics (RCSB, http://www.rcsb.org).

2D structures of the metal complexes were drawn using "Chem Sketch" software. Molegro Virtual Docker was employed[19] for this purpose to analyze compound binding, at specific cavity for both proteins BSA and PTP-1B (PDB ID: 4F5S and 2HNP) respectively. The accuracy of MVD is higher compared with other stock software such as Glide, Sorflex and FlexX.[20] The structure of protein loaded on to MVD platform for finding potential active sites or cavities. BSA consists of 583 amino acid residues present in three homologous alpha helical-domains (I, II, III). Each domain comprises subdomain A and subdomain B.[21,22] On the other hand, PTPs with 321 amino acids is a monomer with one unique protein chain A consisting of alpha helix, beta-strands, and coils.[23] Five binding cavities obtained from site map were employed in reporting the scoring functions. The lead targets were identified based on the scoring functions like Mol dock score. The accuracy of the data was further analyzed by Plant score functionality.

2.2.4 | In vivo studies of metal complexes on Wistar rats

Protocols are followed for in vivo studies of Vanadium metal complexes on Wistar Rats. All animal experiments were conducted as per guidelines of the International Council for Laboratory Animal Science (ICLAS). Efforts were also taken in a direction to minimize animal sufferings, and only the necessary number of animals was used
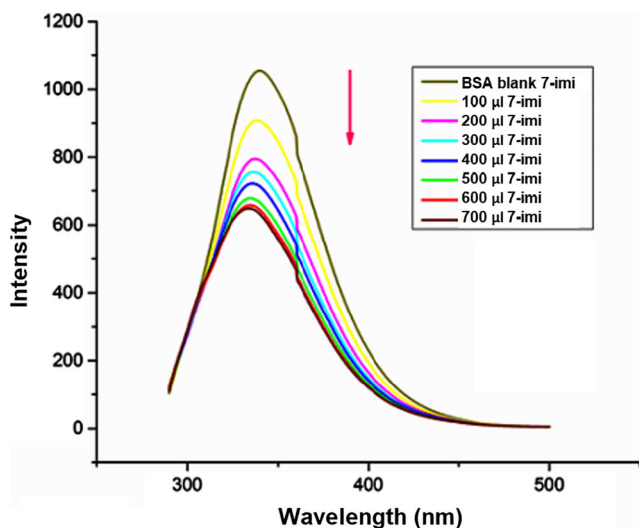
FIGURE 2 Fluorescence emission spectra of bovine serum albumin (BSA) in the absence and presence of different concentrations of [7-imi] complex
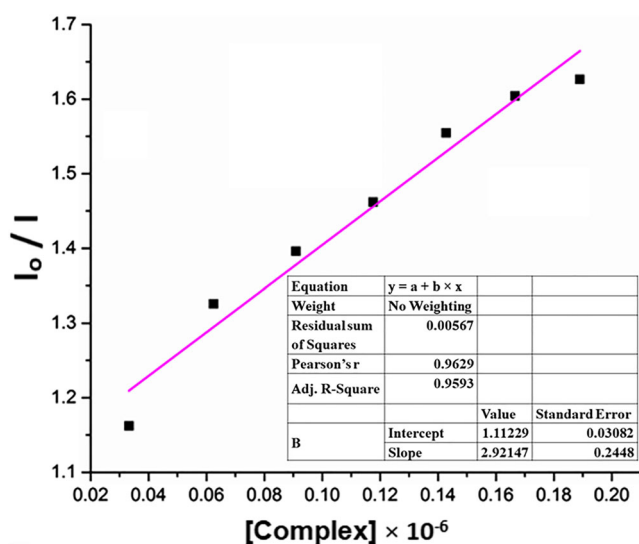

FIGURE 4 The double logarithmic plots for bovine serum albumin (BSA) and [7-imi] complex

FIGURE 3 Stern–Volmer curve for binding of BSA with [7-imi] Intensity values (I) recorded at $\lambda_{max} = 340$ nm

FIGURE 5 Time Vs OD graph for hydrolysis of pNPP in presence of PTP-1B enzyme (40 nM) at different substrate concentrations

to produce reliable scientific data. The *Streptozotocin* (STZ)-diabetes rats were used in the study since they offer a reproducible and reliable test for in vivo insulin-mimetic behaviors.

Induction of diabetes in subjects

Diabetes was induced with STZ (from sigma) 60 mg kg^{-1} in 0.9% NaCl by intravenous tail vein injections under a light halothane anesthesia. The diabetes state was confirmed 3 days following the STZ injection by a blood glucometer test and rats with a blood glucose level $\geq$ 13 mM shall be diagnosed as diabetes.
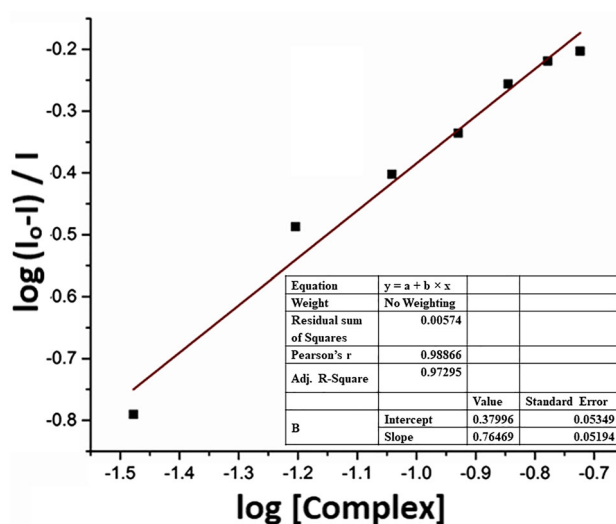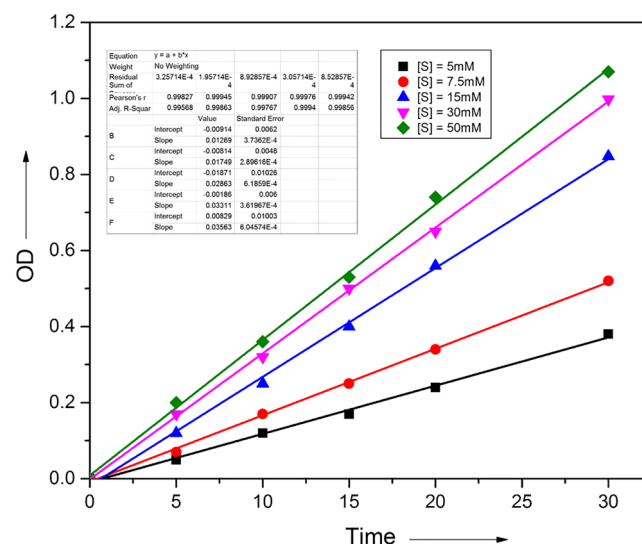
Animal Trials: In all trails, the rats were grouped into seven groups of six animals each and treated. The groups were as labeled below

Group-I: Negative control (NC) (Nondiabetic, normal healthy rats)

Group-II: Positive control (PC) (untreated, Induced diabetic rats)

Group-III: Control treated (CT) (treated with metformin, 1 mg/rat/day)

Group IV: This group of diabetic rats treated with Vanadium metal complexes
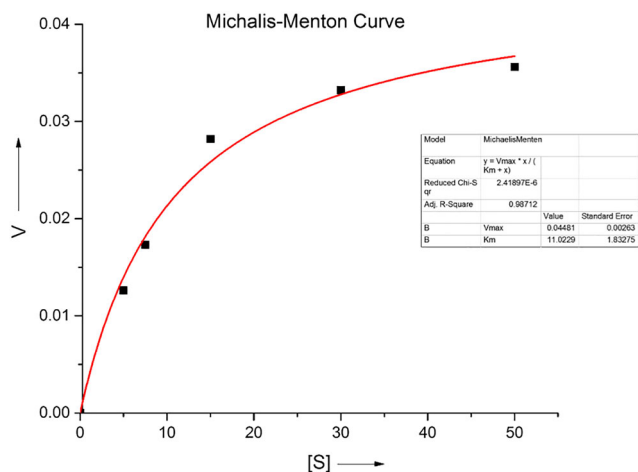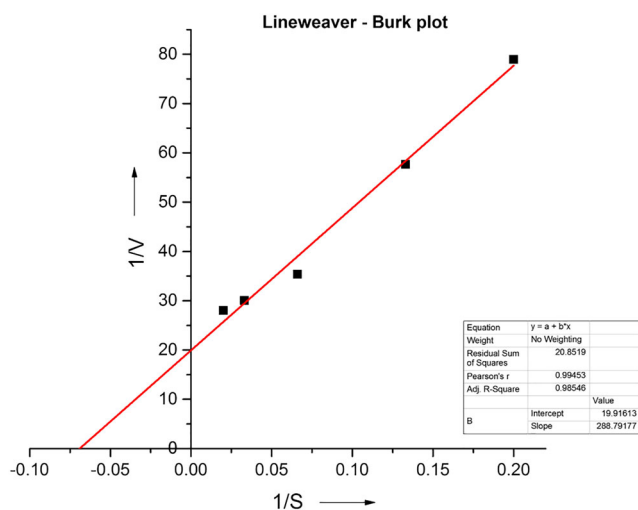
FIGURE 6 Michaelis–Menten curve

FIGURE 7 Lineweaver–Burk plot of pure enzyme

a. Group treated with [7-imi]
b. Group treated with [7-me-imi]
c. Group treated with [7-et-imi]
d. Group treated with [7-B]

Diabetes was induced in all groups except negative control by a single intraperitoneal (IP) injection of 65 mg/Kg body weight of STZ dissolved in freshly prepared 0.1 M Citrate buffer (pH = 4.5). After 72 h, blood was withdrawn from the tail vein of all the rats to check the onset of diabetes in the rats and the blood glucose levels were estimated. To check the effectiveness of vanadium complexes on diabetes, 10 μl in solution form was administered daily (orally) by gastric intubation to the rats in groups IVa to IVd up to 28 days. The standard anti-diabetic drug (Metformin, 1 mg/rat) was administered to group-III rats for 28 days. Blood glucose levels were estimated every week. The plasma glucose estimations were done using a digital glucometer (consisting of a digital

meter and test strips) using blood samples obtained from the tail vein of the rats. Treatment was stopped after the 28th day. Glucose levels were recorded from the 28th day to the 43rd day of the project.

Histopathological studies

The lipid profile along with plasma glucose was also estimated every week which include total cholesterol (TC), serum LDL, serum HDL, serum triglycerides, the ratio of LDL, and HDL. At the end of the experiment period, all animals were physically anesthetized by chloroform inhalation. A midline incision was performed at the thoracic region by a veterinary pathologist. The organs were dissected out, weighed, and filled in 10% formalin saline for the process of histopathology.

3 | RESULTS AND DISCUSSION

3.1 | BSA binding studies by fluorescence technique

The spectrum recorded for [BSA-7-imi] as a representative case is shown in Figure 2. The remaining compounds' spectra are given in Figures S1–S6. Experimental results obtained for various metal complexes for interaction with BSA are is presented in Table S5. The Figure 2 shows that there is a regular decrease in the emission intensity of BSA with an increase in the concentration of vanadium metal complex indicates an interaction takes place between BSA and vanadium metal complex. The extent of interaction can be estimated by calculating the Stern–Volmer constant, quenching rate constant, and binding constant using following equations.

The fluorescence quenching is described by the Stern–Volmer equation[24,25]

$$I_o/I = 1 + K_{sv}[Q] = 1 + k_q \tau_0 [Q] \qquad (1)$$

where I_o is fluorescence intensity of BSA, I is fluorescence intensity of BSA in presence of metal complex, K_{SV} = Stern–Volmer quenching constant, [Q] = concentration of quencher (metal complexes), k_q = bimolecular quenching rate constant of BSA, and τ_0 = Average life time of the biomolecules (BSA) in absence of quencher, generally, its value is 10^{-8} s[26]; the value for BSA is more precisely[27] estimated as 5×10^{-9} s.

a. Calculation of Stern–Volmer quenching constant (K_{sv})

A linear curve obtained in Figure 3 by plotting a graph between [I_o/I] Vs [Q] is suggesting involvement of a single type of quenching mechanism (either static or

TABLE 1 Absorbance values recorded by micro plate reader for hydrolysis of substrate by PTP-1B enzyme in presence of [7-imi] inhibitor

| Time (min) | Concentration of substrate (pNPP) | | | | |
	5 mM	7.5 mM	15 mM	30 mM	50 mM
0	0	0	0	0	0
10	0.061	0.075	0.094	0.193	0.221
20	0.115	0.162	0.186	0.372	0.505
30	0.156	0.215	0.241	0.6	0.87

*Note*: $T = 27°C$, buffer = Tris (pH = 7.5), E = 40 nM, [I] = 5 μM.
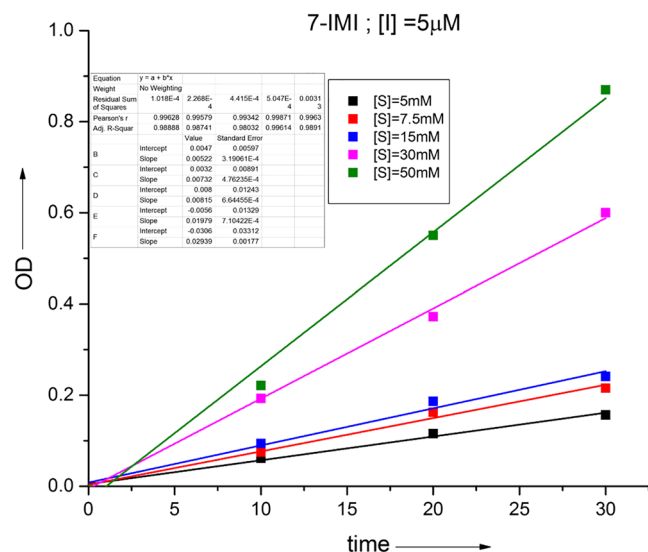
FIGURE 8 Time Vs OD graph for [7-imi] at different substrate concentrations
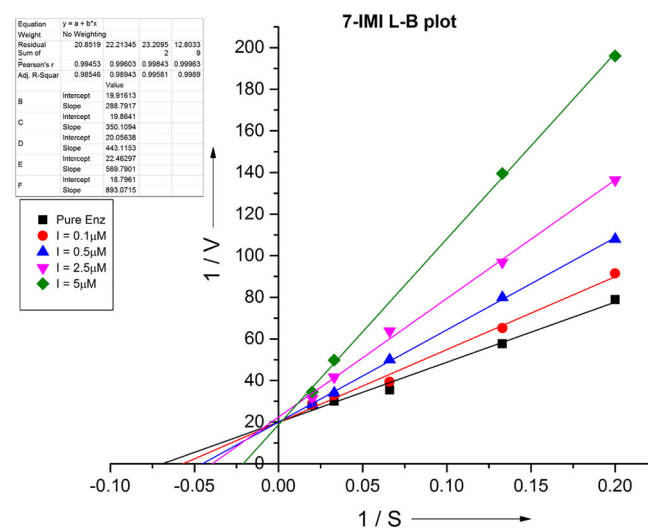
FIGURE 9 L-B plot of the enzyme at different concentrations of inhibitor [7-imi]

dynamic). In the case of [BSA-7-imi] complex, slope and intercept values are 2.921 and 1.112, respectively.

TABLE 2 Comparison of V_{max}, K_m with $K_{m(app)}$ and $V_{max(app)}$ for hydrolysis of pNPP by PTP-1B enzyme

Complex	$V_{max(app)}$ (V_{max}) (mM sc^{-1})	$K_{m\ (app)}$ (K_m) (mM)
[7-imi]	0.0534 (0.050)	52.63 (14.5)

Note: $T = 27°C$, buffer = Tris (pH = 7.5), E = 40 nM, [7-imi] = 10 μM. Values in parenthesis are without inhibitor.
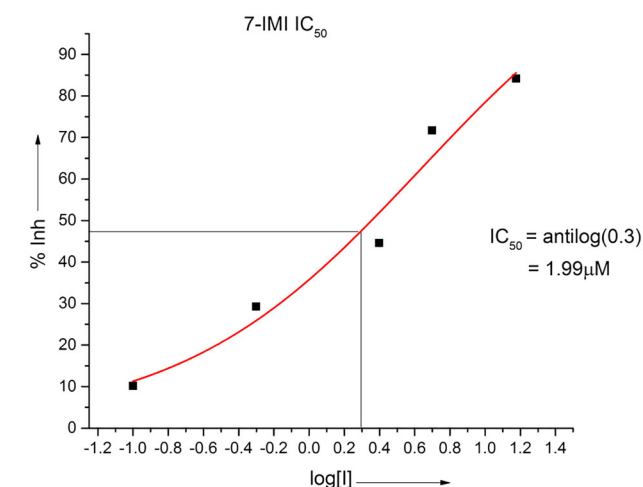
FIGURE 10 Log [I] Vs % inhibition gives IC$_{50}$ values of [7-imi]

Therefore, for [7-imi], slope = K_{sv} = 2.92×10^6 M^{-1}. The K_{SV} values with 10^5 M^{-1} are considered to be indicative of a relatively strong interaction between BSA and metal complexes.

b. Calculation of quenching rate constant (k_q)

The Stern–Volmer quenching constant is given by

$$K_{SV} = (k_q) \times \tau_0 \qquad (2)$$

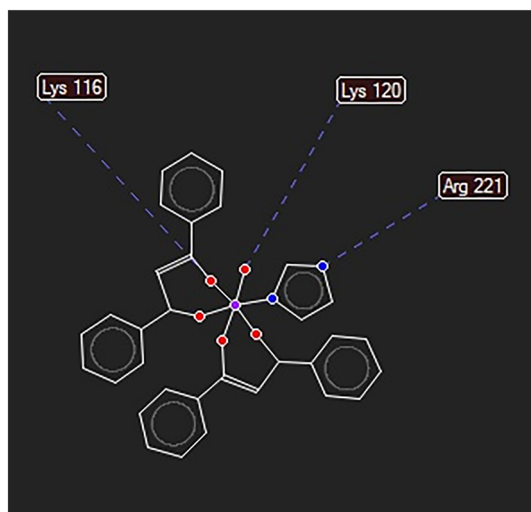k_q (quenching rate constant) values are calculated using the following equation.

$$k_q = K_{SV}/\tau_0 \qquad (3)$$

TABLE 3 Summary of kinetic parameters (from L-B plots) on the hydrolysis of pNPP by PTP-1B enzyme in presence of different inhibitors

S. no	Inhibitors	$V_{max(app)}$	$K_{m(app)}$	dG (KJ)	K_i (μM)	$\frac{K_i}{K_m}$	IC_{50}	Mode of inhibition
1	[7-B]	0.049	50.00	−7.471	1.5532	0.107	3.16	Competitive
2	[7-imi]	0.052	52.63	−7.344	0.9781	0.067	1.99	Competitive
3	[7-me-imi]	0.0516	62.05	−6.915	1.4156	0.098	2.88	Competitive
4	[7-et-imi]	0.0500	50.00	−7.471	1.1256	0.078	2.29	Competitive

TABLE 4 Binding affinity of inhibitors (vanadium metal complexes) to PTP-1B based on Plants, MolDock, and Reranking scores at cavity 1

S. no	Complex	Plants score	MolDock score	Rerank score
1	[7-imi]	−81.6045	−128.711	−79.1859
2	[7-me-imi]	−76.7183	−115.075	−91.0184
3	[7-et-imi]	−78.99	−130.782	−94.3242
4	[7-B]	−74.7142	−143.11	−88.3915

FIGURE 11 Active site of enzyme interaction picture of PTP-1B with [7-imi]

K_{SV} values are divided by 5×10^{-9} s to get quenching rate constant.

$$k_q = 2.92 \times 10^6 \, M^{-1} / 5 \times 10^{-9} s$$

If the k_q value is more than $10^{10} \, M^{-1} \, s^{-1}$ (standard), the suggested mechanism is a static otherwise it is dynamic.[28] In our present study, the k_q values obtained are in the order $10^{15} \, M^{-1} \, s^{-1}$. It concludes that complexation between BSA and Vanadium is static and single type of quenching mechanism.

c. Calculation of binding constants (Kb) and no. of binding sites

The Scatchard equation is given in Equation (4)

$$\log \left[(I_o - I)/I \right] = \log \left[K_b \right] + n \log \left[Q \right] \quad (4)$$

I_o & I are the fluorescence intensity of BSA in the absence and presence of the metal complex. K_b is the binding constant, "n" is the number of binding sites, and [Q] is a concentration of quencher.[29] A graph (Figure 4) is plotted between log (I_o-I/I) Vs log [Q]; a straight line is obtained. The intercept value is a log of K_b. Therefore, antilog of intercept gives the K_b value as 0.379 is $2.34 \times 10^6 \, M^{-1}$. The slope value for BSA is found to be 0.764 which suggests that there is only one binding site available.

Using K_b values, the free energy change (ΔG^o) associated with the formation of [BSA-vanadium] metal complexes is computed using Equation (5).

$$\Delta G^o = -RT \ln K_b \quad (5)$$

The negative values (Table S5) are obtained for all the systems studied indicating the spontaneity of binding.[30]

3.2 | Enzyme kinetics

3.2.1 | Calculation of V_{max} and K_m for hydrolysis of pNPP in presence of PTP-1B

The plots were drawn between absorbance and time intervals, a straight line was obtained. Similar types of lines were seen for different concentrations of substrate, shown in Figure 5. From these plots, the calculated rate constants are presented in Table S6. Using these different rate constants for different concentration of substrate, Michaelis–Menten (M–M) plots (rectangular hyperbola) were drawn between rate Vs [S] and shown in Figure 6.

S. no	Compound	Plants score	MolDock score	Rerank score
1	[7-B]	−75.9075	−97.2944	−77.0017
2	[7-imi]	−80.074	−131.204	−75.2863
3	[7-et-imi]	−79.4278	−108.386	−74.5589
4	[7-me-imi]	−78.1773	−127.746	−71.2719

TABLE 5 Binding affinity of inhibitors (vanadium metal complexes) to BSA based on Plants, Mol Dock, and Reranking scores at cavity 1
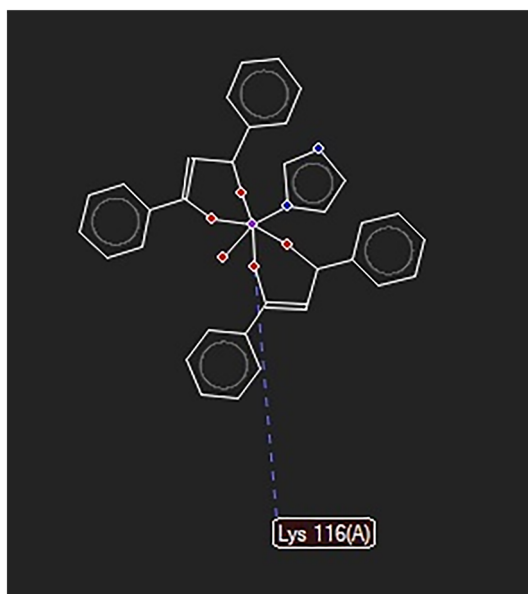

FIGURE 12 Active site of enzyme interaction picture of bovine serum albumin (BSA) with [7-imi]

Lineweaver–Burk (L–B) plots (1/rate Vs 1/[S]) were also plotted from data in Table S7 and presented in Figure 7. L–B plots (also called double reciprocal plots) are the most widely used for linearizing the data and they give the most precise values[31,32] of V_{max} and K_m.

3.2.2 | Calculation of $V_{max(app)}$ and $K_{m(app)}$ for hydrolysis of pNPP in presence of PTP-1B and inhibitor

The obtained OD values with time intervals are listed in Table 1. Time Vs OD graph is plotted, shown in Figure 8, to measure the rate of reaction as described earlier. The M-M and L-B plots are shown in Figures S7 and S8 respectively. Likewise, same experiment was repeated for different concentrations of inhibitor ([7-imi] = 0.5, 2.5, 5 μM). The obtained OD values with time intervals at different concentrations of inhibitor are shown in Table S10. Obtained L-B plots were shown in Figure 9. And the remaining inhibitors' data, M–M and L–B plots, are given in Tables S11–S13 and Figures S9–S14.

The measured $V_{max(apparent)}$ and $K_{m(apparent)}$ values are given in Table S14. Comparison of the values from Table 2

reveals that V_{max} is unaffected and K_m values are affected. Hence, the Vanadium complex [7-imi] affects the rate of the reaction, therefore it is an inhibitor and the type of inhibition is competitive. The measured values of $K_{m(app)}$ and $V_{max(app)}$ for different Vanadium complexes are given in Table S15. All the Vanadium complexes understudy shows unaffected values of V_{max} and affected values of K_m suggesting competitive inhibition.

3.2.3 | Calculation of IC_{50}

The half-maximal inhibitory concentration (IC_{50}) is a measure of the effectiveness of a substance in inhibiting a specific biological or biochemical function. A graph is drawn between Log [I] (on the *x*-axis) and % Inhibition (on the *y*-axis). About 50% of maximal inhibition (IC_{50}) is calculated from the graph (Figures 10 and S15–S17).

3.2.4 | Calculation of inhibition constant (K_i)

The inhibition constants K_i for each inhibitor were calculated[33] using the following equation:

$$K_i = \frac{[IC_{50}]}{1 + \frac{[S]}{K_m}}$$

where IC_{50} = half-maximal inhibitory concentration, K_m = Michaelis–Menten constant without inhibitor, [S] = Concentration of substrate, and K_i = Inhibition constant (dissociation constant). The inhibition constant for [7-imi] is found as 3.09×10^{-6} M or 3.09 μM.

3.2.5 | Discussion

The rate of reaction values in presence of Inhibitor (*I*) is less than in absence of *I*, given in Table S16. This observation suggests the inhibitory action of vanadium metal complex [7-imi].

$V_{max(apparent)}$ and $K_{m(apparent)}$ values are compared with V_{max} and K_m, and it is found that the values of V_{max} and $V_{max(app)}$ are the same, unlike K_m and $K_{m(app)}$ values.

Response					
	Sum of squares	df	Mean square	*F*	Sig.
Between groups	48433.595	10	4843.359	108.183	000
Within groups	2462.344	55	44.770		
Total	50895.938	65			

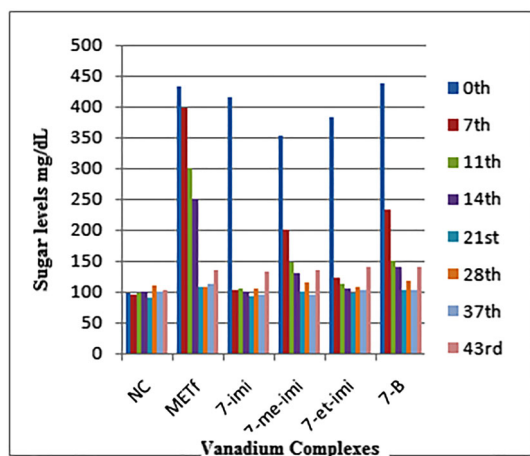Abbreviation: ANOVA, analysis of variance.

FIGURE 13 Trend of sugar levels in *Streptozotocin* (STZ)-induced diabetic rats treated with various vanadium metal complexes during 43 days.

This type of behavior suggests that binding is competitive.[34] It is well-known that in the presence of a competitive inhibitor, the reaction can acquire its $V_{max(app)}$ value equal to V_{max} value. $K_{m(app)}$ however will differ from K_m because $K_{m(app)}$ needs more substrate concentration. Therefore, $K_{m(app)}$ values will be always higher[35] than K_m values and is observed in our present investigation. Experimentally determined value suggests competitive inhibition for all vanadium complexes under study.

The ratio of $\frac{K_i}{K_m}$ directly corresponds to the binding constant for both I and S towards E.

In the present studies, the ratio of $\frac{K_i}{K_m}$ was found to be less than 1 for all the inhibitors under study. Similar types of graphs were obtained for all other inhibitors, and their K_i values are listed in Table 3.

3.2.6 | Type of inhibition exerted on PTP-1B by inhibitor

To know more about the type of Inhibition, the following experiments were conducted.[36] Different concentrations of inhibitor were prepared (0.5, 2.5, 5, 10, and 25 μM); different concentrations of S were prepared (5, 7.5, 15, 30,

and 50 mM). Enzyme concentration was kept constant at 40 nM. A grid of solutions was prepared at each different concentration of substrate by varying concentrations of inhibitor at fixed (40 nM) enzyme concentration. Absorbencies were recorded after terminating reaction wells at 0, 10, 20, and 30 min intervals by adding NaOH. Absorbance at 405 nm was measured using a microplate reader.

L–B plots were drawn and shown in Figure 9. This plot showed a family of lines intercepting on the $\frac{1}{V}$ axis, suggesting a competitive inhibition.

3.3 | Molecular modeling studies of vanadium complexes with enzyme PTP-1B and BSA

3.3.1 | Molecular modeling studies on PTP-1B

Analysis of the docking score for 2HNP reveals that the binding affinity of the molecules is more towards the cavity site-1 (Vol = 84.48). The mol dock score and the plant scores of compounds with PTP-1B at site-1 are provided in Table 4. The 2HNP molecule showed three hydrogen bonds with amino acid residues Lys 116, Lys 120, and Arg 221 in the case of [7-imi] as shown in Figure 11. As a result, a higher binding capacity of 2HNP was reported for [7-imi] compared with the remaining vanadium complexes during docking. [7-imi] secondary structures, hydrogen bond interactions, and detected cavities images after docking are shown in Figures S18 and S19.

3.3.2 | Molecular modeling studies on BSA

The 3D structure of the protein was downloaded from PDB 1D: 4F5S. Analysis of dock score for BSA reveals that the binding affinity of the complexes is more towards the cavity site-1 (Vol = 8539.14) as compared with the other cavities. Site-1 and site-4 correspond to drug binding site I and site II. The mol dock score and the plant scores of compounds with BSA at site-1 are provided in
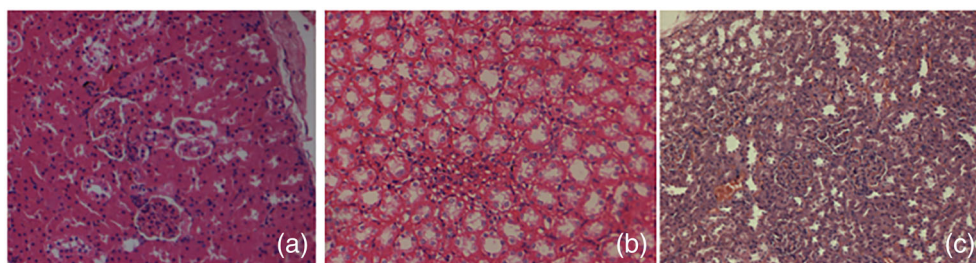
FIGURE 14
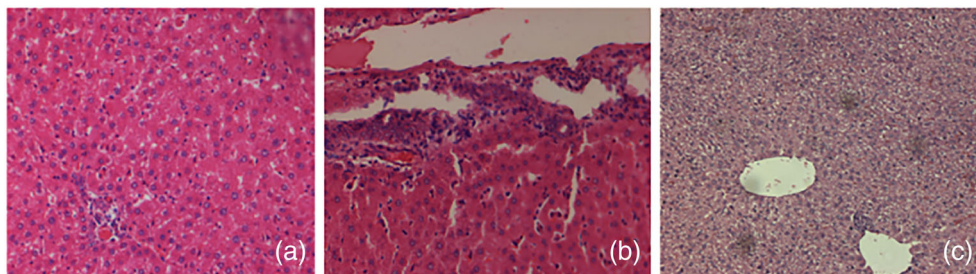Histopathological changes in kidney of healthy rat, diabetic rat, and [7-imi] treated diabetic rats, respectively

FIGURE 15
Histopathological changes in liver of healthy rat, diabetic rat, and [7-imi] treated diabetic rats, respectively
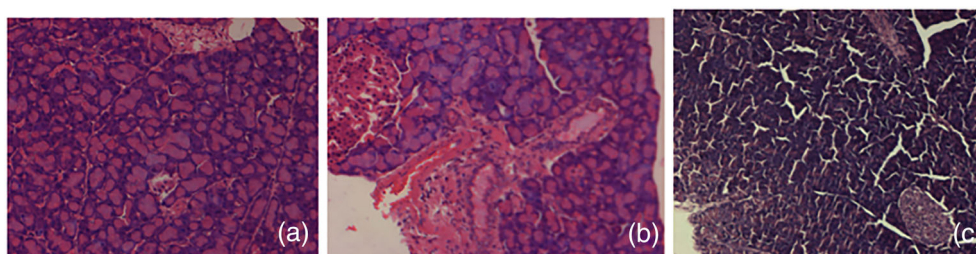

FIGURE 16
Histopathological changes in pancreas of healthy rat, diabetic rat, and [7-imi] treated diabetic rats, respectively

Table 5. The BSA molecule showed only one hydrogen bond interaction with amino acid residues Lys 116 in the case of [7-IMI] as shown in Figure 12. No specific electrostatic and hydrophobic interactions were seen. The higher binding capacity of BSA was reported for [7-IMI] compared with the rest of the metal complexes as a result of a docking simulation. [7-IMI] secondary structures, hydrogen bond interactions, and detected cavities images after docking are shown in Figures S20 and S21.

3.4 | Effect of vanadium complexes on reducing serum glucose levels in induced diabetic Wistar rats

3.4.1 | Statistical analysis

Results (blood glucose levels estimated from a blood sample) were analyzed by using the software "SPSS version 21" and expressed as MEAN $\pm$ SEM. The difference between the groups was tested by one-way analysis of variance (ANOVA), given in Table 6, followed by Tukey's Posthoc test, shown in Table S17. Results were considered significantly different if $p < 0.05$.

Recorded sugar levels in each group and between groups were analyzed using ANOVA followed by Tukey's Posthoc test. The obtained data are presented in Table S18 which is represented in graphical form in Figure 13. Analysis of data or graph reveals that vanadium metal complexes proved to be much better in reducing serum glucose levels when compared with the drug (Metformin) available in the market. The interesting finding is that no rat was found hypoglycemic. The order of sugar reducing property of these six vanadium complexes is as follows

$$[7-\mathrm{Imi}] > [7-\mathrm{et}-\mathrm{imi}] > [7-\mathrm{me}-\mathrm{imi}] > [7-\mathrm{B}]$$
$$> \mathrm{Metformin}$$

3.4.2 | Effect of vanadium complexes on kidney, liver, and pancreas of treated diabetic rats

Histopathology of kidney, liver, and pancreas was studied in normal, diabetic, and treated groups.

Kidney

The normal rat kidney section shows the well-arranged cells and central vein; also, no inflammation and degeneration was noticed. In the diabetic group, haemorrhages and inflammatory cells were noticed. In the [7-imi] treated group, no inflammation was noticed, and histopathological changes are restored near to normal in the kidney treated rats, shown in Figure 14. [7-B] is shown in Figure S22.

Liver

The normal rat Liver section shows the well-arranged cells; also, hepatocytes appeared normal. No inflammation, degeneration, and haemorrhage were noticed. In the diabetic group, moderate to severe inflammation of Liver was noticed. In the [7-imi] treated group, hepatocytes appeared normal; histopathological changes are restored near to normal in the liver of [7-imi] treated rats, as shown in Figure 15. [7-B] is shown in Figure S23.

Pancreas

The normal rat pancreas section shows no degeneration, inflammation, and necrosis. In the diabetic group, moderate to severe necrosis of the pancreas was noticed. In the [7-imi] treated group, the pancreas appeared normal; histopathological changes are restored near to normal in the pancreas of [7-imi] treated rats, as shown in Figure 16. [7-B] is shown in Figure S24.

4 | CONCLUSION

Enzyme inhibitors are usually combined with the enzyme to form in enzyme-inhibitor complex, either by reducing or completely inhibiting the catalytic activity of the enzyme and therefore reducing the rate of reaction. The binding of an inhibitor to the active site of the enzyme can block the entry of the substrate. Overactive enzymes are usually attractive targets for the development of inhibitor molecules to alleviate disease conditions.

The inhibitory action of various vanadium metal complexes on PTP-1B enzyme was studied and found that they have excellent inhibitory properties. We have also studied the interaction of vanadium metal complexes with BSA. To further confirm, we relied on molecular modeling studies. The order of inhibition (Kinetics), the order of binding (binding constant), and results of molecular modeling concerning various vanadium complexes are in consistent with each other. Among these, complex [4-imi] is found to be the best for further studies.

Excited with these results, we conducted animal studies. Based on experimental observations, it is concluded that vanadium metal complexes help in reducing serum glucose levels in animals. They behave as inhibitors to suppress the overexpression of PTP-1B enzyme. The inhibition is competitive. Among these complexes, the complex [7-imi] is found to be the best for further studies. An interesting finding is that no rat was found to be hypoglycemic. However, further studies are required to establish their effect on human beings.

CONFLICT OF INTEREST

The authors declare that there is no conflict of interest.

AUTHOR CONTRIBUTIONS

Ayub Shaik: Data curation; formal analysis; investigation; supervision; validation; visualization. **Vani Kondaparthy:** Data curation; formal analysis. **Rambabu Aveli:** Data curation. **Louwkhyaa Vemulapalli:** Data curation; investigation. **Devadas Manwal:** Conceptualization; methodology; resources; validation.

DATA AVAILABILITY STATEMENT

The data that support the findings of this study are available in the supporting information of this article.

ORCID

Ayub Shaik https://orcid.org/0000-0003-2000-9347
Vani Kondaparthy https://orcid.org/0000-0001-8895-7410
Rambabu Aveli https://orcid.org/0000-0001-8356-0035
Louwkhyaa Vemulapalli https://orcid.org/0000-0001-9313-5796
Deva Das Manwal https://orcid.org/0000-0002-3473-6548

REFERENCES

[1] B. Lyonnet, M. Martz, E. Martin, *La Presse Med.* **1899**, *1*, 191.

[2] K. Cusi, S. Cukier, R. A. DeFronzo, M. Torres, F. M. Puchulu, J. C. P. Redondo, *J. Clin. Endocrinol. Metab.* **2001**, *86*, 1410.

[3] Y. Niu, W. Liu, C. Tian, M. Xie, L. Gao, Z. Chen, X. Chen, L. Li, *Eur. J. Pharmacol.* **2007**, *572*(2–3), 213. https://doi.org/10.1016/j.ejphar.2007.05.071

[4] a) R. Mukherjee, E. G. Donnay, M. A. Radomski, C. Miller, D. A. Redfern, A. Gericke, D. S. Damron, N. E. Brasch, *Chem. Commun.* **2008**, 3783; b) K. H. Thompson, J. Lichter, C. LeBel, M. C. Scaife, J. H. McNeill, C. Orvig, *J. Inorg. Biochem.* **2009**, *103*, 554; c) L. Lu, S. Wang, M. Zhu, Z. Liu, M. Guo, *Biometals* **2010**, *23*, 1139; d) A. B. Goldfine, D. C. Simonson, F. Folli, M. E. Patti, C. R. Kahn, *J. Clin. Endocrinol. Metab.* **1995**, *80*, 3311; e) A. B. Goldfine, D. C. Simonson, F. Folli, M. E. Patti, C. R. Kahn, *Mol. Cell. Biochem.* **1995**, *153*, 217; f) N. Cohen, M. Halberstam, P. Shlimovich, C. J. Chang, H. Shamoon, L. Rossetti, *J. Clin. Investig.* **1995**, *95*, 2501; g) G. Boden, X. Chen, J. Ruiz, G. Van Rossum, S. Turco, *Metabolism* **1996**, *45*, 1130; h) M. W. Makinen, M. J. Brady, *J. Biol. Chem.* **2002**, *277*(14), 12215. https://doi.org/10.1074/jbc.M110798200

[5] S. Ayub, K. Vani, M. D. Das, *J. Applicable Chem.* **2018**, *7*, 1223.

[6] A. Shaik, V. Kondaparthy, R. Aveli, M. Vijjulatha, S. S. Kanth, D. D. Manwal, *Inorg. Chem. Commun.* **2021**, *126*, 108499.

[7] L. Lu, S. Wang, M. Zhu, Z. Liu, M. Guo, S. Xing, X. Fu, *Biometals* **2010**, *23*(6), 1139. https://doi.org/10.1007/s10534-010-9363-8

[8] A. Cheng, N. Dube, F. Gu, M. L. Tremblay, *Eur. J. Biochem.* **2002**, *269*(4), 1050. https://doi.org/10.1046/j.0014-2956.2002.02756.x

[9] K. Shi, K. Egawa, H. Maegawa, T. Nakamura, *J. Biochem.* **2004**, *136*, 89. https://doi.org/10.1093/jb/mvh094

[10] D. J. Pagliarini, F. L. Robinson, C. A. Worby, J. E. Dixon, *Encyclopedia of Biological Chemistry*, Elsevier Inc **2013**, 648. https://doi.org/10.1016/B978-0-12-378630-2.00366-2

[11] G. Huyer, S. Liu, J. Kelly, J. Moffat, P. Payette, B. Kennedy, G. Tsaprailis, M. J. Gresser, C. Ramachandran, *J. Biol. Chem.* **1997**, *272*, 843. https://doi.org/10.1074/jbc.272.2.843

[12] E. Bellomo, K. B. Singh, A. Massarotti, C. Hogstrand, W. Maret, *Coord. Chem. Rev.* **2016**, *327–328*, 70. https://doi.org/10.1016/j.ccr.2016.07.002

[13] A. S. Tracey, G. R. Willsky, E. S. Takeuchi, *Vanadium: Chemistry, Biochemistry, Pharmacology, and Practical Applications*, 1st ed., CRC Press **2007**. https://doi.org/10.1201/9781420046144

[14] E. Irving, A. W. Stoker, *Molecules* **2017**, *22*(12), 2269. https://doi.org/10.3390/molecules22122269

[15] M. Anjomshoa, S. J. Fatemi, M. T. Mahani, *Spectrochim. Acta A Mol. Biomol. Spectrosc.* **2014**, *127*, 511. https://doi.org/10.1016/j.saa.2014.02.048

[16] J. Korbecki, I. Baranowska-Bosiacka, I. Gutowska, D. Chlubek, *Acta Biochim. Pol.* **2012**, *59*, 195. https://doi.org/10.18388/abp.2012_2138

[17] Q. Wang, L. Lu, C. Yuan, K. Pei, Z. Liu, M. Guo, M. Zhu, *Chem. Commun.* **2010**, *46*, 3547.

[18] C. Yuan, L. Lu, X. Gao, Y. Wu, M. Zhu, *J. Biol. Inorg. Chem.* **2009**, *14*(6), 841. https://doi.org/10.1007/s00775-009-0496-6

[19] A. Molegro, MVD 5.0 Molegro Virtual Docker. DK-8000 Aarhus C, Denmark **2011**.

[20] L. Liu, H. Ma, N. Yang, Y. Tang, J. Guo, *Thromb. Res.* **2010**, *126*, 365.

[21] K. A. Majorek, P. J. Porebski, A. Dayal, M. D. Zimmerman, K. Jablonska, A. J. Stewart, M. Chruszcz, W. Minor, *Mol. Immunol.* **2012**, *52*(3–4), 174. https://doi.org/10.1016/j.molimm.2012.05.011

[22] A. Bujacz, *Biol. Crystallogr.* **2012**, *68*, 1278.

[23] N. Pinotsis, G. Walsman, *J. Biol. Chem.* **2017**, *292*(22), 9240. https://doi.org/10.1074/jbc.M117.781948

[24] M. A. Jhonsi, A. Kathiravan, R. Ranganathan, *Colloids Surf.* **2009**, *72*, 167. https://doi.org/10.1016/j.colsurfb.2009.03.030

[25] J. R. Lakowicz, *Principles of Fluorescence Spectroscopy*, 3rd ed., Springer, Newyork **2006**. https://doi.org/10.1007/978-0-387-46312-4

[26] Y. Q. Wang, H. M. Zhang, G. C. Zhang, W. H. Tao, *J. Mol. Struct.* **2007**, *830*(1–3), 40. https://doi.org/10.1016/j.molstruc.2006.06.031

[27] G. Scatchard, *Ann. N. Y. Acad. Sci.* **1949**, *51*(4), 660. https://doi.org/10.1111/j.1749-6632.1949.tb27297.x

[28] J. R. Lakowicz, *Principles of Fluorescence Spectroscopy*, 2nd ed., Springer, New York **2004**.

[29] P. Sathyadevi, P. Krishnamoorthy, R. R. Butorac, A. H. Cowley, N. S. P. Bhuvanesh, N. Dharmaraj, *Dalton Trans.* **2011**, *40*(38), 9690. https://doi.org/10.1039/c1dt10767d

[30] S. Roy, T. K. Das, *Adv. Mat. Lett.* **2015**, *11*, 1018. https://doi.org/10.5185/amlett.2015.5933

[31] J. Montalibet, K. I. Skorey, B. P. Kennedy, *Methods* **2005**, *35*(1), 2. https://doi.org/10.1016/j.ymeth.2004.07.002

[32] T. Palmer, P. L. Bonner, *Enzymes: Biochemistry, Biotechnology, Clinical chemistry*, Elsevier **2007** https://doi.org/10.1533/9780857099921

[33] C. G. Whiteley, *Biochem. Educ.* **2000**, *28*, 144. https://doi.org/10.1016/S0307-4412(00)00029-7

[34] Q. Wu, L. Jiang, S. Yang, Y. Zuo, Z. Wang, Z. Xi, G. Yang, *New J. Chem.* **2014**, *38*(9), 4510. https://doi.org/10.1039/C4NJ00636D

[35] J. M. Berg, J. L. Tymoczko, L. Stryer, *Biochemistry*, 5th ed., W. H. Freeman Publishing **2002** ISBN-10:0–7167–3051–3050.

[36] L. R. Engelking, *Enzyme Kinetics, Textbook of Veterinary Physiological Chemistry*, **2015** 32 https://doi.org/10.1016/B978-0-12-391909-0.50006-2

SUPPORTING INFORMATION

Additional supporting information may be found in the online version of the article at the publisher's website.